

See discussions, stats, and author profiles for this publication at: <https://www.researchgate.net/publication/322169068>

# Thermogravimetric Analysis of Textile Dyeing Sludge (TDS) in N<sub>2</sub>/CO<sub>2</sub>/O<sub>2</sub> Atmospheres and its Combustion Model with ....

Article in *Water Environment Research* · January 2018

DOI: 10.2175/106143017X15054988926514

CITATIONS

2

READS

25

7 authors, including:



**Jing-Yong Liu**

GuangDong University of Technology

90 PUBLICATIONS 507 CITATIONS

[SEE PROFILE](#)



**Jian Sun**

Zhejiang University

381 PUBLICATIONS 35,464 CITATIONS

[SEE PROFILE](#)

Some of the authors of this publication are also working on these related projects:



Thermodynamic [View project](#)



electrochemical ORR catalyst [View project](#)

# Thermogravimetric Analysis of Textile Dyeing Sludge (TDS) in N<sub>2</sub>/CO<sub>2</sub>/O<sub>2</sub> Atmospheres and its Combustion Model with Coal

Zhongxu Zhuo<sup>1</sup>, Jingyong Liu<sup>1,2\*</sup>, Shuiyu Sun<sup>1</sup>, Jiahong Kuo<sup>1,2</sup>, Jian Sun<sup>1,2</sup>, Ken-Lin Chang<sup>1,2</sup>, Jiewen Fu<sup>1</sup>

**ABSTRACT:** The combustion characteristics of textile dyeing sludge (TDS) in N<sub>2</sub>/O<sub>2</sub>, CO<sub>2</sub>/O<sub>2</sub>, and N<sub>2</sub>/CO<sub>2</sub> atmospheres, and blends of TDS with coal were analyzed using TGA (thermogravimetric analysis). Results showed that the replacement of N<sub>2</sub> by CO<sub>2</sub> resulted in negative effects on the combustion and pyrolysis of TDS. Comparing N<sub>2</sub>/O<sub>2</sub> and CO<sub>2</sub>/O<sub>2</sub> atmospheres, combustion of TDS was easier in a N<sub>2</sub>/O<sub>2</sub> atmosphere, but the residual mass after TDS pyrolysis in pure CO<sub>2</sub> was less than that in N<sub>2</sub> by approximately 4.51%. When the proportion of TDS was 30–50% in the blends of coal with TDS, a synergistic interaction clearly occurred, and it significantly promoted combustion. In considering different combustion parameters, the optimal proportion of TDS may be between 20–30%. The activation energy  $E_a$  value decreased from 155.6 kJ/mol to 53.35 kJ/mol with an increasing TDS proportion from 0% to 50%, and it rapidly decreased when the TDS proportion was below 20%. *Water Environ. Res.*, 90, 30 (2018).

**KEYWORDS:** textile dyeing sludge (TDS), coal, oxy-fuel combustion, thermogravimetric analysis, kinetics.

doi:10.2175/106143017X15054988926514

## Introduction

Textile dyeing wastewater is characterized by strong color and high concentration of suspended solids. During the treatment process for textile dyeing, wastewater and large amounts of sludge are generated (dos Santos et al., 2007). In textile dyeing sludge (TDS), inert solids, polymer solids, precipitated dyes, metal salts and other chemicals are the main pollutants which cause serious environmental pollution if inappropriately treated (Patel and Pandey, 2012). To dispose of

TDS efficiently, landfill and incineration are the two main methods used in China. However, with shrinking landfill space and continually rising environmental consciousness, the proportion of landfill in TDS treatment will gradually decrease. Rather, the role of incineration will increase in the future for its volume reduction, stabilization, sanitation, and energy generation (Zhang et al., 2008), which has been demonstrated in many European countries (Kelessidis and Stasinakis, 2012).

Because traditional combustion technology results in only approximately 14% CO<sub>2</sub> in the flue gas, it is difficult and expensive to capture CO<sub>2</sub> from the flue gas (Singh et al., 2003). The cost of gas separation can be reduced by increasing the concentration of CO<sub>2</sub> in the flue gas. In fact, a commercial scaled pyrolysis plant must also be operated under an oxygen free atmosphere. Thus, combustion and pyrolysis in a CO<sub>2</sub> enriched atmosphere was suggested as one of the new promising technologies for capturing CO<sub>2</sub> from power plants (Lai et al., 2012b; Selcuk and Yuzbasi, 2011). Molina and Shaddix (2007) found that replacement of N<sub>2</sub> by CO<sub>2</sub> can cause significant differences in incinerator operation parameters such as burning stability, char burnout, heat transfer and gas temperature. Chen et al. (2007) found that the CO<sub>2</sub> concentrations in the flue gas under CO<sub>2</sub>/O<sub>2</sub> and O<sub>2</sub>/recycled atmospheres were much higher than that in a N<sub>2</sub>/O<sub>2</sub> atmosphere, whereas the NO<sub>x</sub> concentration in N<sub>2</sub>/O<sub>2</sub> combustion was higher than that in CO<sub>2</sub>/O<sub>2</sub> or O<sub>2</sub>/recycled fuel gas combustion. Duan et al. (2009) reported that replacing N<sub>2</sub> with CO<sub>2</sub> could increase the SO<sub>2</sub> release rate. Lai et al. (2012a) found that replacement of 80% N<sub>2</sub> by 80% CO<sub>2</sub> influenced combustion negatively, and an oxygen content of 30% in the CO<sub>2</sub>/O<sub>2</sub> atmosphere achieved a combustion performance similar to that in N<sub>2</sub>/O<sub>2</sub>=80/20. However, few studies involved the differences among the combustion characteristics of TDS in N<sub>2</sub>/O<sub>2</sub>, CO<sub>2</sub>/O<sub>2</sub> and N<sub>2</sub>/CO<sub>2</sub> atmospheres.

<sup>1</sup> School of Environmental Science and Engineering, Guangdong University of Technology, Guangzhou 510006, China

<sup>2\*</sup> Institute of Environmental Health and Pollution Control, Guangdong University of Technology, Guangzhou 510006, China; e-mail: www053991@126.com (J. Y. Liu)

**Table 1—The ultimate and proximate analyses of air dried TDS and coal.**

Sample	Ultimate analyses (%wt)					Proximate analyses (%wt)			
	C	H	N	S	O	M <sup>a</sup>	V <sup>b</sup>	A <sup>c</sup>	FC <sup>d</sup>
TDS	24.2	6.08	3.22	2.76	25.35	11.70	44.71	36.04	7.55
coal	62.61	5.3	1.15	0.87	9.3	10	29.05	13.59	47.36

<sup>a</sup> M, moisture<sup>b</sup> V, volatile matters<sup>c</sup> A, ash<sup>d</sup> FC, fixed carbon

In China, reserves of coal are more abundant than those of natural gas and raw petroleum. In primary energy consumption, coal plays an important role in China's energy usage and accounts for 70% approximately. In the long term, coal will still make a great contribution to China's economic growth (Sun et al., 2014). In principle, energy policy promotes the use of biomass and locally generated waste as fuel to support the carbon economy (Otero et al., 2007). Previous researchers (Peng et al., 2015a) found a synergistic interaction between microalgae and TDS in co-combustion, which could avoid the drawbacks of each fuel and improve their combustion performance. The co-combustion of TDS with coal, under appropriate control, may be a secure method, and it may also generate profits through energy recovery. TDS has a smaller fixed carbon content, which leads to a lower calorific value (Cong et al., 2013). However, it has very high levels of volatile matter compared with coal. Thus, the co-combustion of coal and TDS could avoid the drawbacks of using two fuels, and it may increase their combustion efficiency. The kinetics parameters and combustion mechanism of the combustion process are also important for pollution control. This information is lacking and unclear, especially for the co-combustion of TDS with coal. Thermogravimetric analysis (TGA) has been widely used in biomass combustion and pyrolysis research as a method of determining combustion, pyrolysis characteristics and kinetic parameters (Lopez-Velazquez et al., 2013; Liu et al., 2016). TGA can provide a valid way to evaluate the kinetics of thermally induced reactions (Otero et al., 2007), therefore, it is necessary to investigate how the addition of TDS alters the kinetics of coal combustion.

Because of the limited knowledge of the combustion and pyrolysis characteristics of TDS, the objective of this work was to experimentally quantify the impact of different atmospheres (N<sub>2</sub>/O<sub>2</sub>, CO<sub>2</sub>/O<sub>2</sub>, and N<sub>2</sub>/CO<sub>2</sub>) for TDS. Although the co-combustion and co-pyrolysis of TDS with microalgae has been studied to some extent (Peng et al., 2015a; Peng et al., 2015b), coal will still make a great contribution to China's economic growth in the long term. Thus, it is necessary to study the combustion characteristics of the blends of TDS and coal under different sludge weight percentages, after which the kinetics parameters were calculated to give an appraisal of the co-combustion of coal with TDS. The results could provide a valuable reference for designing and optimizing combustion and pyrolysis technologies for TDS.

## Methodology

**Materials.** Samples of TDS were collected from the Dongguan Chao Ying Textile Co., Ltd. (Guangdong Province, China), and coal was collected from Yulin, Shanxi Province. The ultimate analysis and proximate analysis of TDS and coal are presented in Table 1 (Zhuo et al., 2017). TDS and coal were dried in natural air for one week and milled through a 200 mesh sieve before use, whereupon all the mixtures were mixed for an hour in a rotary mixer. After the above treatment, the samples were stored in a desiccator for testing.

**Experimental Facility and Procedure.** Thermogravimetry tests were carried out on a NETZSCH STA409PC simultaneous analyzer. To eliminate the effects of mass and heat transfer limitations, small samples (9.5–10.5 mg) were loaded into an Al<sub>2</sub>O<sub>3</sub> ceramic crucible for each run under non isothermal conditions. The small sample in the reactor was heated up from ambient temperature to 1000 °C with a heating rate of 20 °C/min. In the experiment, TGA was employed to investigate the combustion characteristics of the TDS in N<sub>2</sub>/O<sub>2</sub>, CO<sub>2</sub>/O<sub>2</sub>, and N<sub>2</sub>/CO<sub>2</sub> atmospheres at different concentration rates with a flow rate of 100 mL/min. In addition, the co-combustion characteristics of TDS and coal were also studied with different proportions of TDS. A separate blank run was conducted for baseline correction after each test, using an empty pan. Furthermore, the experiments were repeated three times to confirm the repeatability and authenticity of the generated data, and the error was measured to be within ± 1% (He and Ma, 2015).

## Results and Discussion

**Pyrolysis and Combustion of TDS in N<sub>2</sub>, CO<sub>2</sub> and O<sub>2</sub> Atmospheres.** TG-DTG (thermal gravity-differential thermal gravity) curves of TDS in N<sub>2</sub>, CO<sub>2</sub>, and O<sub>2</sub> atmospheres at a heating rate of 20 °C/min are presented in Figure 1. As shown in Figure 1, TDS lost little weight from ambient temperature to approximately 120–150 °C under N<sub>2</sub>, CO<sub>2</sub>, and O<sub>2</sub> atmospheres, corresponding to a loss of moisture and a small amount of volatile material. In N<sub>2</sub> and CO<sub>2</sub> atmospheres, the temperature of the second weight loss stage (volatile release) began at 120 °C and 150 °C, then it ended at 480 °C and 750 °C, respectively.

In the N<sub>2</sub> atmosphere, a more discernible weight loss region existed in the temperature range of 480–900 °C compared with that in the CO<sub>2</sub> atmosphere, corresponding to the thermal decomposition of calcium carbonate and other minerals (Liao

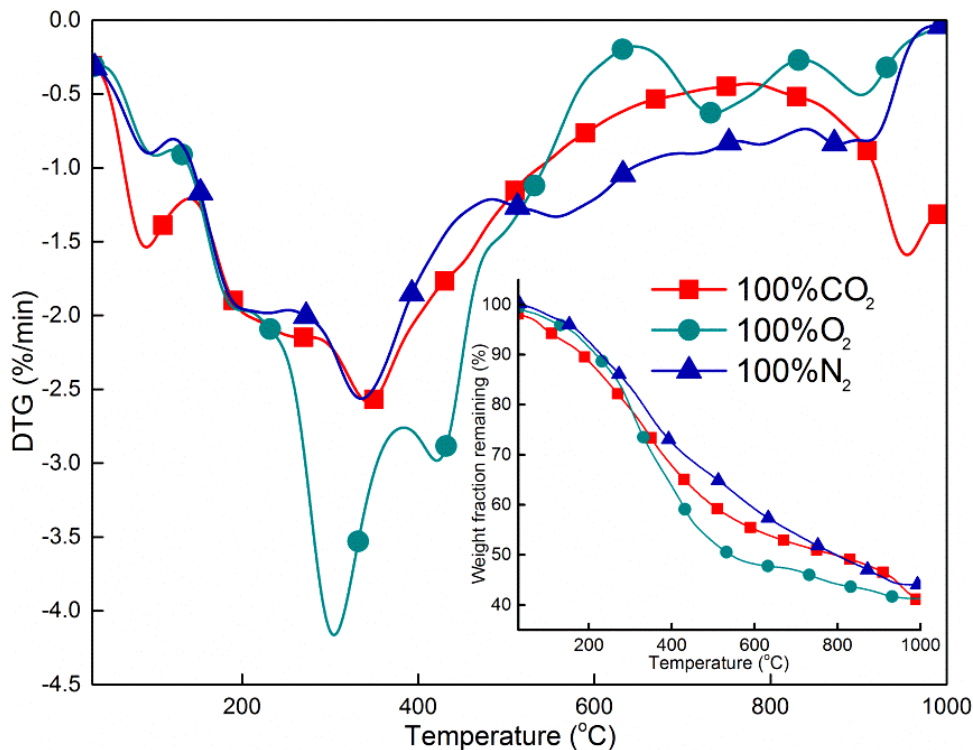


**Figure 1—TG-DTG curves of TDS in  $N_2$ ,  $CO_2$ , and  $O_2$  atmospheres at 20 °C/min.**

and Ma, 2010). In the  $CO_2$  atmosphere, the DTG curve showed a peak above 900 °C due to the char gasification that did not occur in a pure  $N_2$  atmosphere.

In the  $O_2$  atmosphere, the second weight loss stage corresponded to the temperature of 120–380 °C, which represented the release and combustion of volatile matter (small molecular weight organic compounds). The third combustion stage, between 380 °C and 640 °C, was attributed to the combustion of macromolecular organic matter in TDS. The fourth stage, from 640–834 °C, corresponded to fixed carbon (FC) combustion. The fifth stage, in a temperature range from 834 to 1000 °C, mainly involved the decomposition of inorganic minerals, such as calcium carbonate, dolomite, and kaolin (Peng et al., 2015b).

**Table 2—Combustion and pyrolysis parameters obtained from TG-DTG curves of TDS under  $N_2$ ,  $CO_2$ , and  $O_2$  atmospheres.**

Conditions	$T_v^a$ (°C)	$T_f^b$ (°C)	$-DTG_{max}^c$ (%/min)	$T_{DTGmax}^d$ (°C)
$N_2$	233.2	918.984	2.56	335.8
$CO_2$	234.5	980.913	2.58	345.1
$O_2$	213.1	889.715	4.16	304.7

<sup>a</sup>  $T_v$ , the onset temperature for volatile release

<sup>b</sup>  $T_f$ , the temperature of 98% conversion

<sup>c</sup>  $DTG_{max}$ , maximum weight loss rate

<sup>d</sup>  $T_{DTGmax}$ , the temperature associated with  $DTG_{max}$

Comparing the pyrolysis process of TDS in  $N_2$  with that in  $CO_2$ , the values of  $T_v$ ,  $T_{DTGmax}$ , and  $DTG_{max}$  showed small differences (Table 2), which indicated that  $CO_2$  had a minor effect on combustion reactions at the initial stage of pyrolysis. The  $T_f$  (temperature at 98% conversion) of TDS in a  $CO_2$  atmosphere was 62 °C higher than that in a  $N_2$  atmosphere. The residual mass was approximately 4.51% less in a  $CO_2$  atmosphere than that in a  $N_2$  atmosphere, which was mainly because the char gasification only occurred in the presence of  $CO_2$ .

**Combustion of TDS under  $N_2/O_2$  and  $CO_2/O_2$  Atmospheres.** Figure 2a,b show the TG-DTG curves of TDS combustion with different oxygen concentrations in the  $N_2/O_2$  and  $CO_2/O_2$  atmospheres at a 20 °C/min heating rate. Five discernible weight loss peaks were found in the DTG curves, which was similar to that in a pure  $O_2$  atmosphere. The main conversion focuses on the temperature of 150–670 °C, taking up approximately 80–85% of the total conversion of TDS. In this stage, the DTG curves of TDS had an analogous trend under  $N_2/O_2$  and  $CO_2/O_2$  atmospheres. With increased oxygen concentration, the DTG curve gradually shifted to the lower temperature, while this trend among 670–1000 °C was unapparent because the content of fixed carbon and inorganic minerals was very small.

Table 3 shows the combustion parameters of TDS under  $N_2/O_2$  and  $CO_2/O_2$  atmospheres. With the increased oxygen concentration, the trend where the values of  $T_v$ ,  $T_f$ ,  $T_2$ ,  $T_3$ ,  $DTG_2$  and  $DTG_3$  changed (listed in Table 3) was the same in both  $N_2/O_2$  and  $CO_2/O_2$  atmospheres. Note that the ranges of

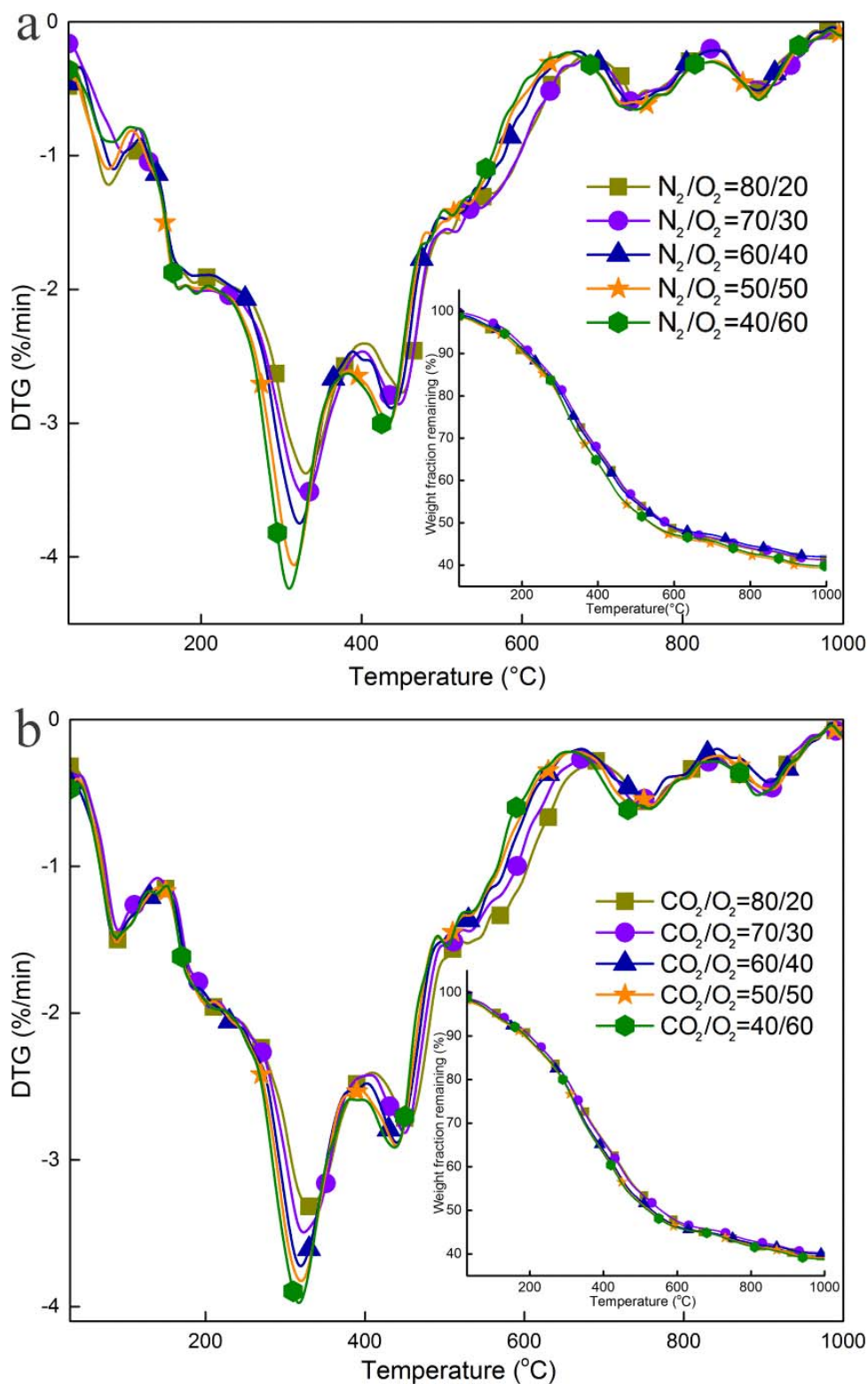


**Figure 2—TG-DTG curves of TDS under different atmospheres at 20 °C/min: (a)  $N_2/O_2$ ; (b)  $CO_2/O_2$ .**

these values under a  $N_2/O_2$  atmosphere were always larger than that under  $CO_2/O_2$ . The values of  $T_v$ ,  $T_f$ ,  $T_2$  and  $T_3$ , were 6.4, 12.7, 22.5, 20.9 and 5.8, 8.4, 11.9, 12.7 in both atmospheres ( $N_2/O_2$  and  $CO_2/O_2$ ) with the proportions of 80/

20 and 40/60, respectively. At the same time,  $DTG_2$  and  $DTG_3$  in the  $N_2/O_2$  atmosphere were larger than those in the  $CO_2/O_2$  atmosphere under all of the corresponding proportions, indicating that, to a certain extent, the replacement of  $N_2$  by

**Table 3—Combustion parameters obtained from TG-DTG curves of TDS under N<sub>2</sub>/O<sub>2</sub> and CO<sub>2</sub>/O<sub>2</sub> atmospheres.**

Conditions	$T_v^a$ (°C)	$T_f^b$ (°C)	$T_2^c$ (°C)	$T_3^c$ (°C)	-DTG <sub>2</sub> <sup>d</sup> (%/min)	-DTG <sub>3</sub> <sup>d</sup> (%/min)
N <sub>2</sub> /O <sub>2</sub> atmosphere						
O <sub>2</sub> =20%	222.5	895.0	332.0	451.6	3.37	2.77
O <sub>2</sub> =30%	220.2	892.4	329.5	447.5	3.54	2.86
O <sub>2</sub> =40%	219.8	889.3	322.5	436.5	3.75	2.88
O <sub>2</sub> =50%	217.7	885.9	315.5	433.9	4.06	2.98
O <sub>2</sub> =60%	216.1	882.3	309.5	430.7	4.24	3.04
CO <sub>2</sub> /O <sub>2</sub> atmosphere						
O <sub>2</sub> =20%	222.6	899.7	329.4	452.2	3.32	2.73
O <sub>2</sub> =30%	220.2	897.1	323.1	449.5	3.49	2.82
O <sub>2</sub> =40%	219.6	896.3	318.5	440.9	3.72	2.87
O <sub>2</sub> =50%	218.3	894.9	320.5	439.7	3.83	2.90
O <sub>2</sub> =60%	216.8	891.3	317.5	439.5	3.97	2.92

<sup>a</sup>  $T_v$ , the onset temperature for volatile release

<sup>b</sup>  $T_f$ , the temperature of 98% conversion

<sup>c</sup>  $T_2$ ,  $T_3$ , the temperature according to the second peak, and the third peak

<sup>d</sup> DTG<sub>2</sub>, DTG<sub>3</sub>, the weight loss rate according to  $T_2$ ,  $T_3$

CO<sub>2</sub> resulted in negative effects on TDS combustion. These effects include lower speed of propagation and stability of the flame and gas temperature under CO<sub>2</sub>/O<sub>2</sub> combustion (Buhre et al., 2005).

**Thermal Decomposition of TDS under N<sub>2</sub>/CO<sub>2</sub> Atmospheres.** To further explore the effects of CO<sub>2</sub> instead of N<sub>2</sub> on TDS pyrolysis, pyrolysis experiments were conducted and the pyrolysis parameters were calculated in N<sub>2</sub>/CO<sub>2</sub> = 80/20, N<sub>2</sub>/CO<sub>2</sub> = 70/30, N<sub>2</sub>/CO<sub>2</sub> = 50/50, and N<sub>2</sub>/CO<sub>2</sub> = 40/60 atmospheres. The TG-DTG curves of TDS at a heating rate of 20 °C/min in different N<sub>2</sub>/CO<sub>2</sub> atmospheres are shown in Figure 3a. Below 500 °C, different N<sub>2</sub>/CO<sub>2</sub> atmospheres had a weak effect on the TG-DTG curves, indicating that the CO<sub>2</sub> instead of N<sub>2</sub> had a slight effect on the release of volatile material. From 500–900 °C, the DTG curves shifted to the lower temperature gradually when CO<sub>2</sub> concentration decreased from 20% to 60%. Over 900 °C, the value of the weight loss peak increased gradually with the increase in CO<sub>2</sub> concentration, as shown in Figure 3b, and the peak was prone to a higher temperature.

The pyrolysis parameters of TDS under different N<sub>2</sub>/CO<sub>2</sub> atmospheres are listed in Table 4. The values of the third weight loss peak in N<sub>2</sub>/CO<sub>2</sub> = 80/20, N<sub>2</sub>/CO<sub>2</sub> = 70/30, N<sub>2</sub>/CO<sub>2</sub> = 50/50, and N<sub>2</sub>/CO<sub>2</sub> = 40/60 were 0.99%/min, 1.06%/min, 1.22%/min, and 1.31%/min, and the corresponding temperatures were 943.239 °C, 945.357 °C, 948.884 °C, and 953.054 °C, respectively. This indicated that the CO<sub>2</sub> had reaction activity under high temperature conditions (Minkova et al., 2000) and that it could react with char. Similar results were found in the thermal decomposition of coal (Li et al., 2009).

**Co-combustion of Coal and TDS.** Figure 4 represents the TG-DTG curves of coal, TDS, and their blends in different ratios at a heating rate of 20 °C/min under N<sub>2</sub>/O<sub>2</sub> = 80/20 at a flow rate of 100 mL/min (parts of the data (coal and 20TDS:80coal have been published (Zhuo et al., 2017)). The TG-DTG of coal had a weight loss peak at the temperature

range of 500–700 °C, and the maximum weight loss rate occurred at 616 °C, after which the residues reached a constant weight of approximately 16% according to the ash content listed in Table 1. All of the TG-DTG curves of the blends of sludge and coal occurred between the individual fuels. As the weight percentage of TDS increased, the combustion evolution profiles of the blends gradually changed from a tendency of coal to that of TDS.

To evaluate the effect of the atmosphere on combustion and pyrolysis, the comprehensive combustion index (CCI) was defined as follows (López-González et al., 2014):

$$CCI = \frac{(dW/dt)_{\max}(dW/dt)_{\text{mean}}}{T_i^2 T_f} \quad (1)$$

where  $(dW/dt)_{\max}$  is the maximum mass loss rate,  $(dW/dt)_{\text{mean}}$  is the average mass loss rate,  $T_i$  is the ignition temperature, and  $T_f$  is the burnout temperature. The larger the CCI was, the more vigorously the samples burned and the faster the char burned out.

The combustion parameters of coal and TDS blends are listed in Table 5. To better understand the relationship between the characteristic parameters and TDSP (the proportion of TDS in the blends), the tendencies of  $T_v$ ,  $T_f$ ,  $M_f$ ,  $T_{\max}$ , -DTG<sub>max</sub> and CCI are illustrated according to TDSP, see Figure 5.

It is clear that the values of  $T_v$ ,  $T_{\max}$ , -DTG<sub>max</sub> and CCI decreased and  $M_f$  increased with increasing TDSP. Moreover, their correlation coefficients ( $R^2$ ) were all between 0.915 and 0.975, except for those of  $T_v$  ( $R^2 = 0.813$ ) and  $T_{\max}$  ( $R^2 = 0.850$ ). The final combustion temperature ( $T_f$ ) decreased when TDSP was below 30%, and it sharply increased when TDSP was over 30%, which indicated that the best TDSP might be below 30% in the co-combustion of coal and TDS. The ratio of 30% was a turning point of flammability for the combustion of the blends, and the blend samples burned out earlier when TDSP was below 30%. Furthermore, the decrease in  $T_{\max}$  of the blends began to flatten when TDSP was over 30%, which suggested that the best

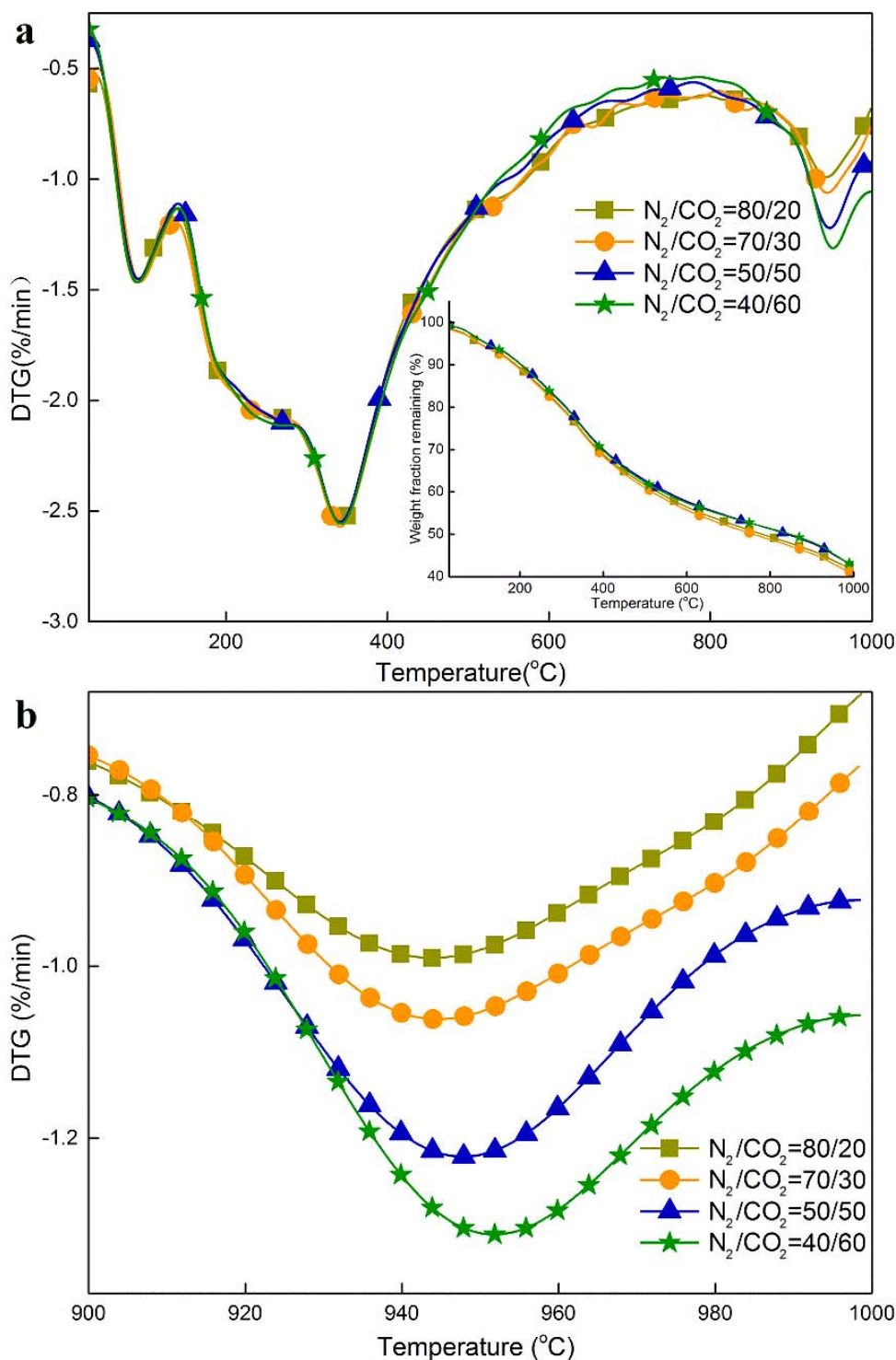


**Figure 3—Pyrolysis of TDS under  $N_2/CO_2$  atmospheres at 20  $^{\circ}C/min$ : (a)  $N_2/CO_2$ ; (b) from 900 to 1000  $^{\circ}C$  under  $N_2/CO_2$  atmospheres.**

TDSP might also be below 30%. The residual mass increased sharply and CCI decreased slowly when TDSP was below 20%. On the whole, the optimal TDSP may be between 20% and 30%.

Assuming that there was no interaction between coal and TDS, the total mass loss of the blends was the average mass of

the individuals, which can be calculated as followed (Aboulkas et al., 2008):

$$W = X_{coal}W_{coal} + X_{TDS}W_{TDS} \quad (2)$$

where  $W_{coal}$  and  $W_{TDS}$  are the corresponding weight fractions remaining of the individual materials, and  $X_{coal}$  and  $X_{TDS}$  are

**Table 4—Pyrolysis parameters obtained from TG-DTG curves of TDS under N<sub>2</sub>/CO<sub>2</sub> atmospheres.**

Conditions	T <sub>v</sub> <sup>a</sup> (°C)	T <sub>f</sub> <sup>b</sup> (°C)	T <sub>3</sub> <sup>c</sup> (°C)	-DTG <sub>3</sub> <sup>d</sup> (%/min)
N <sub>2</sub> /CO <sub>2</sub> = 80/20	233.1	969.439	943.239	0.99
N <sub>2</sub> /CO <sub>2</sub> = 70/30	235.8	971.157	945.357	1.06
N <sub>2</sub> /CO <sub>2</sub> = 50/50	232.3	974.284	948.884	1.22
N <sub>2</sub> /CO <sub>2</sub> = 40/60	231.5	977.254	953.054	1.31

<sup>a</sup> T<sub>v</sub>, the onset temperature for volatile release

<sup>b</sup> T<sub>f</sub>, the temperature of 98% conversion

<sup>c</sup> T<sub>3</sub>, the temperature according to the second peak, and the third peak

<sup>d</sup> DTG<sub>3</sub>, the weight loss rate according to T<sub>3</sub>

the proportions of the coal and TDS in the blends. The experimental and calculated TG curves when TDSP was at 5%, 10%, 20%, 30%, 40%, and 50% are shown in Figure 6.

As shown in Figure 6, when the temperature was lower than 500 °C, the calculated thermal gravity curves corresponded well with the experimental thermal gravity curves (except at 50% TDSP). A gap existed between the experimental and calculated TG curves when the temperature was over 500 °C, especially at 50% TDSP. The results indicate that a synergistic interaction occurred in the co-combustion of coal and TDS, which has also been demonstrated by other studies (Liao and Ma, 2010). At 30%, 40% and 50% TDSP, the gap between the experimental and calculated TG curves at the temperature range of 500–670

°C was discernible, and it indicated that blending coal with TDS promoted combustion efficiency.

**Combustion Kinetics Model.** *Kinetics Parameters.* Kinetics parameters are very important in revealing the reaction mechanism of co-combustion. The parameters deduced from the TG-DTG curves include the reaction model ( $f(\alpha)$ ), the pre-exponential factor ( $A$ ), the activation energy ( $E_a$ ) and the reaction order ( $n$ ) (Otero et al., 2007). In general, the thermal degradation of a solid-state sample can be simply shown as:  $B_{\text{solid}} \rightarrow C_{\text{solid}} + D_{\text{gas}}$ , where  $B_{\text{solid}}$  is the initial material, and  $C_{\text{solid}}$  and  $D_{\text{gas}}$  are the different products during the disappearance of  $B_{\text{solid}}$ . In thermogravimetric measurements, the degree of decomposition (conversion) can be calculated as follows:

$$\alpha = \frac{M_0 - M_t}{M_0 - M_\infty} \quad (3)$$

where  $M_0$ ,  $M_t$  and  $M_\infty$  are the weights of the sample before combustion, at time  $t$  during combustion, and at the end of the reaction. The relative amount of feedstock remaining at any time is hence  $(1 - \alpha)$ . The reaction rate constant is defined by the Arrhenius equation:

$$k = Ae^{-E_a/RT} \quad (4)$$

where  $k$  is the reaction rate constant (in s<sup>-1</sup>) for a first order reaction (or in appropriate units as a function of the conversion model used),  $E_a$  is the activation energy (J/mol), and  $A$  is the pre-exponential factor (in units of  $k$ ).

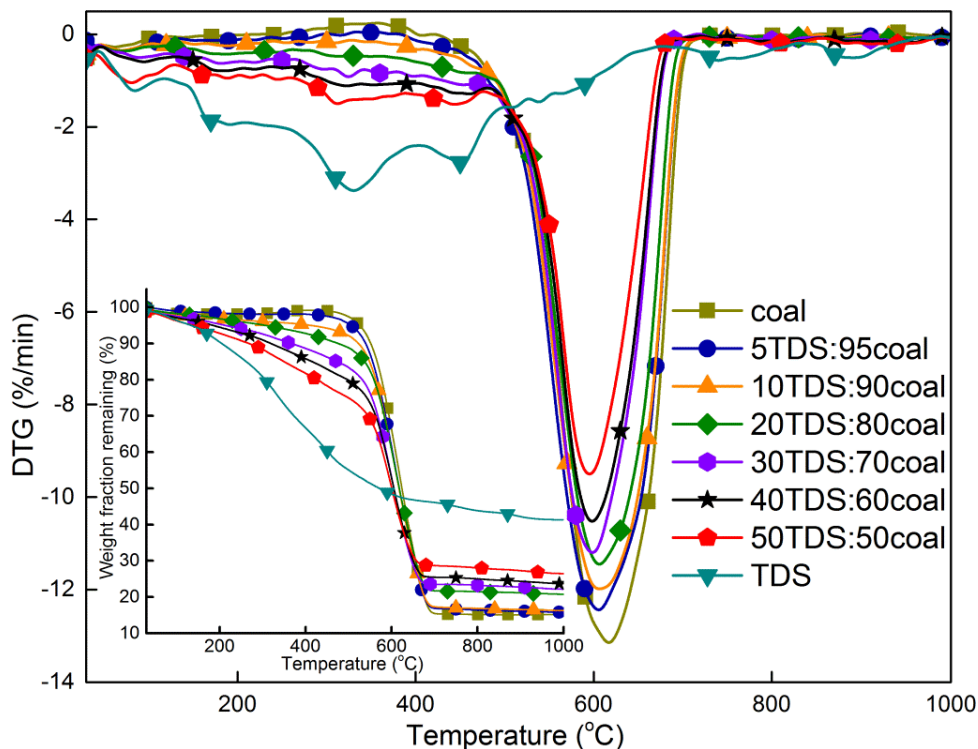


**Figure 4—TG-DTG curves of TDS, coal, and their blends under an 80N<sub>2</sub>/20O<sub>2</sub> atmosphere at 20 °C/min (Zhuo et al., 2017).**

**Table 5—Combustion parameters obtained from TG-DTG curves of TDS, coal, and their blends under a N<sub>2</sub>/O<sub>2</sub> = 80/20 atmosphere.**

Samples	T <sub>v</sub> <sup>a</sup> (°C)	T <sub>f</sub> <sup>b</sup> (°C)	-DTG <sub>max</sub> <sup>c</sup> (%/min)	T <sub>DTGmax</sub> <sup>d</sup> (°C)	M <sub>f</sub> <sup>e</sup> (%)	CCI <sup>f</sup> (10 <sup>7</sup> )
coal	550.1	689.3	13.14	617.7	15.12	1.54
5TDS:95coal	542.2	688.8	12.40	606.4	15.76	1.48
10TDS:90coal	540.3	685.7	11.98	607.3	16.27	1.44
20TDS:80coal	536.3	682.7	11.44	605.7	20.79	1.34
30TDS:70coal	534.8	678.8	11.19	598.7	22.18	1.30
40TDS:60coal	533.1	770.5	10.52	597.3	23.72	0.94
50TDS:50coal	532.3	815.6	9.50	594.8	26.45	0.73

<sup>a</sup> T<sub>v</sub>, the onset temperature for volatile release

<sup>b</sup> T<sub>f</sub>, the temperature of 98% conversion

<sup>c</sup> DTG<sub>max</sub>, maximum weight loss rate

<sup>d</sup> T<sub>DTGmax</sub>, the temperature associated to DTG<sub>max</sub>

<sup>e</sup> M<sub>f</sub>, the residual mass

<sup>f</sup> CCI, the comprehensive combustion index

As the weight of the sample is continuously registered, M<sub>0</sub>, M<sub>t</sub> and M<sub>∞</sub> are defined and the reaction rate constant can be derived at every moment because the known heating rate of the TGA relates the temperature ramp to the timescale. The Arrhenius equation can be applied after data transformation and plotting of the results in a function of the reaction mechanism.

In the non-isothermal TGA experiments, the weight of the sample is measured as a function of temperature, whereas the reaction proceeds for a fixed regime of temperature ramps β (K/min). The degradation can thus also be expressed as a function of time, t, because ΔT and Δt are linked in the experiments. The rate of degradation, or conversion, dα/dt, is a function of the temperature dependent rate constant, k, and a temperature independent function of conversion, f(α). The resulting equation is:

$$\frac{d\alpha}{dt} = k \cdot f(\alpha) \quad (5)$$

The rate constant, k, can be described by the Arrhenius expression in eq 4. The overall expression of the reaction rate takes the form of:

$$\frac{d\alpha}{dt} = k \cdot f(\alpha) = A e^{-E_a/RT} f(\alpha) \quad (6)$$

During the experiments, β = dT/dt was used. The conversion, α, can thus be written as a function of the temperature, T:

$$\frac{d\alpha}{dt} = \frac{d\alpha}{dT} \frac{dT}{dt} = \beta \frac{d\alpha}{dT} \quad (7)$$

The combination of eqs 6 and 7 results in the following expression:

$$\frac{d\alpha}{dt} = \frac{A}{\beta} e^{-E_a/RT} f(\alpha) \quad (8)$$

Integration and recombination of eq. 8 yields (Ebrahimi-Kahrizsangi and Abbasi, 2008):

$$G(\alpha) = \int_0^\alpha \frac{d\alpha}{f(\alpha)} \int_0^T e^{-E_a/RT} dT \quad (9)$$

where G(α) represents the integrated form of the conversion dependence, but without a specific analytical solution. Several

expressions for G(α) have been proposed in the literature as a function of different reaction mechanisms, all of which are based on three concepts: diffusion, nucleation, and the order of the reaction. Expressions of G(α) were summarized from previous literature (Bianchi et al., 2008; Chen and Wang, 2007). These models differ only in considering the rate limiting step to be either diffusion, nucleation, or the reaction itself.

Using x as E<sub>a</sub>/RT, eq 9 can be rewritten in a more useable form:

$$p(x) = \int_x^\infty \frac{e^{-x}}{x^2} dx \quad (10)$$

G(α) can then be solved as (Chen and Wang, 2007):

$$G(\alpha) = \frac{AE_a}{\beta R} \int_x^\infty \frac{e^{-x}}{x^2} dx = \frac{AE_a}{\beta R} p(x) \quad (11)$$

The integral method uses the Doyle approximation (Doyle, 1962) of the temperature integral given in eq 12.

$$\ln G(\alpha) = \ln\left(\frac{AE_a}{\beta R}\right) - 5.3305 - 1.052 \frac{E_a}{RT} \quad (12)$$

By plotting the left hand side of the equation versus 1/T, the activation energy, E<sub>a</sub>, can be determined from the slope of the linear expression.

To evaluate the kinetics parameters A, E<sub>a</sub>, and n, the residual sum of squares (RSS) is commonly used as the accordance criterion of the theoretical and experimental curves. It is defined as the following relationship:

$$RSS = \sum_{i=1}^{\theta} (\alpha_{ci} - \alpha_{ei})^2 \quad (13)$$

where α<sub>ei</sub> is the degree of conversion of a specimen in the point i of the TG curve, and α<sub>ci</sub> is the value calculated at the corresponding point. The lowest RSS values are obtained for the best parameter estimates.

Figure 7a,b (Zhuo et al., 2017) gives an example for explaining the method to determine the best model for coal at the active combustion stage, which covers nearly 95% of the weight loss process. Twelve models available in Figure 7a were

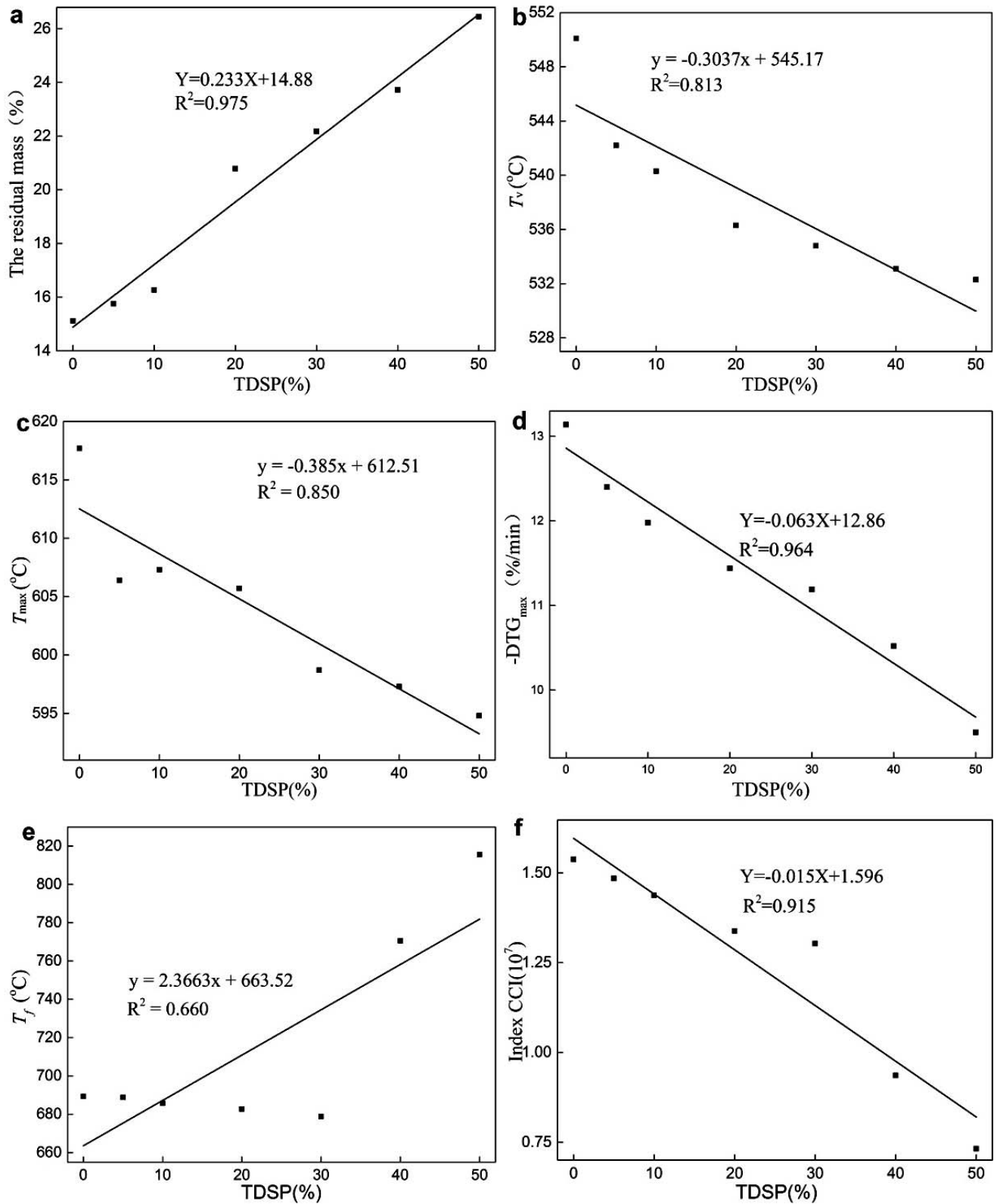


**Figure 5—The relationship between different parameters and TDSP: (a) the relationship between  $M_f$  and TDSP; (b) the relationship between  $T_v$  and TDSP; (c) the relationship between  $T_{max}$  and TDSP; (d) the relationship between  $-DTG_{max}$  and TDSP; (e) the relationship between  $T_f$  and TDSP; (f) the relationship between the index CCI and TDSP.**

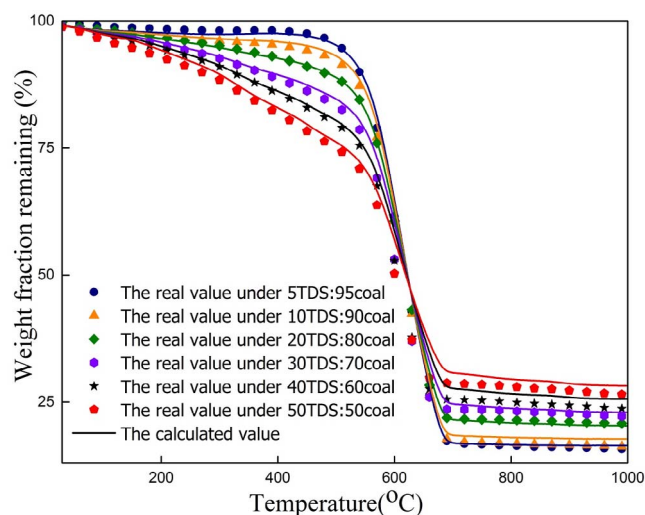


**Figure 6—The comparison of experimental and calculated thermal gravity curves of blends.**

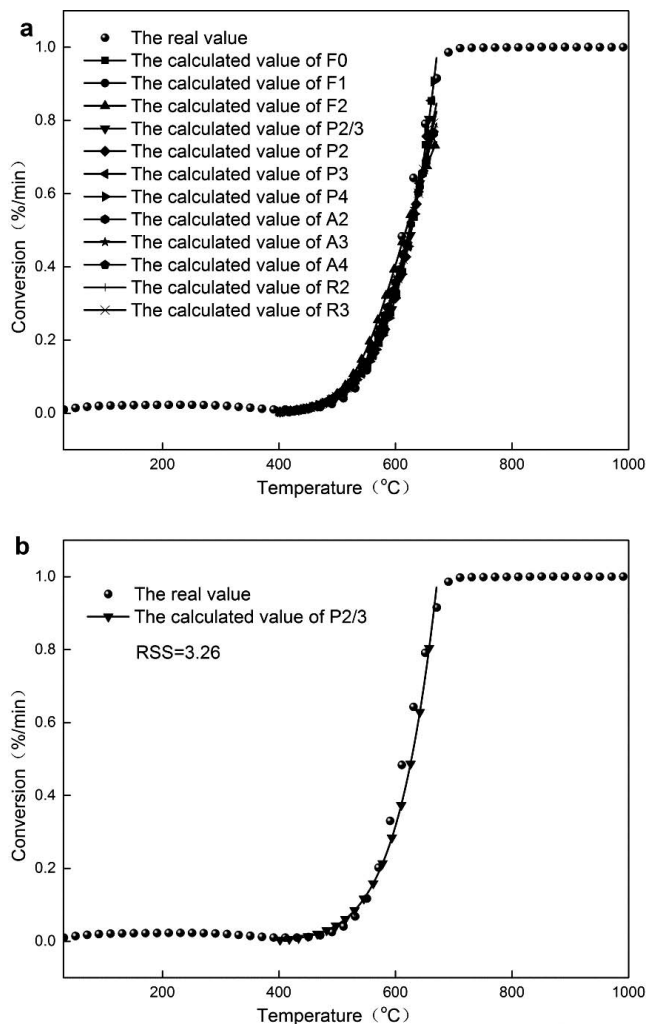
used to calculate the RSS, where the smallest value corresponds to the best fitting model, as shown in Figure 7b.

Table 6 reports the best kinetics parameters obtained from the direct non linear regression of various kinetics expressions to the experimental data and the corresponding RSS. Among the models above, the P(2/3) model, as shown in Figure 7b, should be the most suitable mechanism function that can describe the kinetics properties for the co-combustion of coal and blends. The activation energy ( $E_a$ ) varies from 155.6 kJ/mol for coal to 53.35 kJ/mol for 50TDS:50coal.

As shown in Figure 8, the relationship between  $E_a$  and TDSP showed that, for the blends, a higher percentage of TDS corresponded to a lower  $E_a$ . The variation of the kinetics parameters occurred because of the complicated composition of TDS, including dyestuff, slurry, dyeing aid, acids or alkalis, fibers, and inorganic compounds (Patel and Pandey, 2012). The compounds that were concentrated in TDS had been broken down by biological oxidation and had a simple structure, and they were easy to decompose at high combustion temperatures. Furthermore,  $E_a$  decreased rapidly when TDSP was below 20%, after which  $E_a$  decreased slowly.

## Conclusions

The replacement of  $N_2$  by  $CO_2$  resulted in negative effects on the combustion and pyrolysis characteristics, and combus-



**Figure 7—Comparison of the models and experimental conversion curves of coal: (a) comparison of the model and experimental conversion curve of coal; (b) the best model for the combustion process of coal (Zhuo et al., 2017).**

tion in a  $N_2/O_2$  atmosphere was made easier by increasing the  $O_2$  content. However, the residual mass was approximately 4.51% less in a pure  $CO_2$  atmosphere than in  $N_2$ . The synergistic interaction occurring in the co-combustion of coal and TDS, especially at 30%, 40%, and 50% TDSP, significantly promoted combustion efficiency when the tem-

**Table 6—The kinetics parameters for combustion of coal and the TDS/coal blends.**

Sample	$\ln A$ ( $s^{-1}$ )	$E_a$ (kJ/mol)	n	$f(\alpha)$	RSS
coal	19.31	155.60	3/2	$2/3\alpha^{-1/2}$	3.26
5TDS:95coal	15.42	125.50	3/2	$2/3\alpha^{-1/2}$	3.84
10TDS:95coal	11.51	95.62	3/2	$2/3\alpha^{-1/2}$	5.33
20TDS:80coal	9.52	79.65	3/2	$2/3\alpha^{-1/2}$	5.46
30TDS:70coal	8.40	68.76	3/2	$2/3\alpha^{-1/2}$	3.97
40TDS:60coal	7.11	58.27	3/2	$2/3\alpha^{-1/2}$	3.58
50TDS:50coal	6.65	53.35	3/2	$2/3\alpha^{-1/2}$	1.85

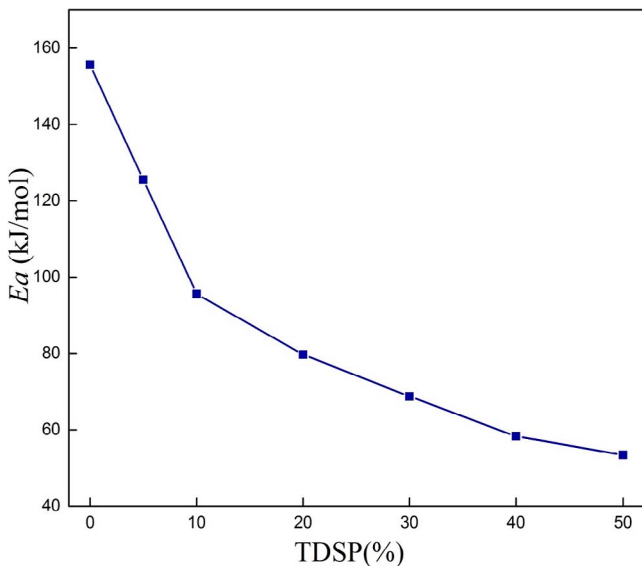


**Figure 8—The relationship between  $E_a$  and TDSP.**

perature range was between 500 and 670 °C. The  $E_a$  value decreased from 155.6 kJ/mol to 53.35 kJ/mol with an increasing TDS ratio, and it rapidly decreased when TDS was below 20%. From the analysis of combustion characteristics and kinetics parameters, the best TDS proportion might be between 20 and 30%.

## Acknowledgements

This work was supported by the Science and Technology Planning Project of Guangdong Province, China (No.2014A050503063; No.2016A040402006; No.2016A040403069; No. 2015B020235013), the Scientific and Technological Planning Project of Guangzhou, China (No.2016201604030058; No. 201704030109) and Guangdong Special Support Program for Training High Level Talents (No.2014TQ01Z248).

Submitted for publication September 2, 2016; revised manuscript submitted March 19, 2017; accepted for publication March 30, 2017.

## References

- Aboulkas, A.; El Harfi, K.; El Bouadili, A. (2008) Pyrolysis of Olive Residue/Low Density Polyethylene Mixture: Part I Thermogravimetric Kinetics. *J. Fuel Chem. Technol.*, **36**, 672–678.
- Bianchi, O.; Oliveira, R.; Fiorio, R.; Martins, J.; Zattera, A.; Canto, L. (2008) Assessment of Avrami, Ozawa and Avrami-Ozawa Equations for Determination of EVA Cross-Linking Kinetics from DSC Measurements. *Polym. Test.*, **27**, 722–729.
- Buhre, B. J. P.; Elliott, L. K.; Sheng, C. D.; Gupta, R. P.; Wall, T. F. (2005) Oxy-Fuel Combustion Technology for Coal-Fired Power Generation. *Prog. Energ. Combust.*, **31**, 283–307.
- Chen, J.; Liu, Z.; Huang, J. (2007) Emission Characteristics of Coal Combustion in Different O<sub>2</sub>/N<sub>2</sub>, O<sub>2</sub>/CO<sub>2</sub> and O<sub>2</sub>/RFG Atmosphere. *J. Hazard. Mater.*, **142**, 266–271.
- Chen, Y.; Wang, Q. (2007) Thermal Oxidative Degradation Kinetics of Flame-Retarded Polypropylene with Intumescent Flame-Retardant Master Batches in situ Prepared in Twin-Screw Extruder. *Polym. Degrad. Stabil.*, **92**, 280–291.

- Cong, S.; Duan, F.; Zhang, Y.; Liu, J.; Zhang, J.; Zhang, L. (2013) O<sub>2</sub> Emission from Municipal Sewage Sludge Cocombustion with Bituminous Coal Under O<sub>2</sub>/CO<sub>2</sub> Atmosphere Versus O<sub>2</sub>/N<sub>2</sub> Atmosphere. *Energy Fuels*, **27**, 7067–7071.
- dos Santos, A. B.; Cervantes, F. J.; van Lier, J. B. (2007) Review Paper on Current Technologies for Decolourisation of Textile Wastewaters: Perspectives for Anaerobic Biotechnology. *Bioresour. Technol.*, **98**, 2369–2385.
- Doyle, C. D. (1962) Estimating Isothermal Life from Thermogravimetric Data. *J. Appl. Polym. Sci.*, **6**, 639–642.
- Duan, L.; Zhao, C.; Zhou, W.; Liang, C.; Chen, X. (2009) Sulfur Evolution from Coal Combustion in O<sub>2</sub>/CO<sub>2</sub> Mixture. *J. Anal. Appl. Pyrol.*, **86**, 269–273.
- Ebrahimi-Kahrizsangi, R.; Abbasi, M. H. (2008) Evaluation of Reliability of Coats-Redfern Method for Kinetic Analysis of Non-Isothermal TGA. *Trans. Nonferrous Met. Soc. China*, **18**, 217–221.
- He, Y.; Ma, X. (2015) Comparative Investigation on Non-Isothermal Kinetics for Thermo Degradation of Lignocellulosic Substrate and its Chlorinated Derivative in Atmospheres with CO<sub>2</sub> Participation. *Bioresour. Technol.*, **189**, 71–80.
- Kelessidis, A.; Stasinakis, A. S. (2012) Comparative Study of the Methods used for Treatment and Final Disposal of Sewage Sludge in European Countries. *Waste Manage.*, **32**, 1186–1195.
- Lopez-Velazquez, M. A.; Santes, V.; Balmaseda, J.; Torres-Garcia, E. (2013) Pyrolysis of Orange Waste: A Thermo-Kinetic Study. *J. Anal. Appl. Pyrol.*, **99**, 170–177.
- López-González, D.; Fernandez-Lopez, M.; Valverde, J. L.; Sanchez-Silva, L. (2014) Kinetic Analysis and Thermal Characterization of the Microalgae Combustion Process by Thermal Analysis Coupled to Mass Spectrometry. *Appl. Energy*, **114**, 227–237.
- Lai, Z.; Ma, X.; Tang, Y.; Lin, H.; Chen, Y. (2012a) Thermogravimetric Analyses of Combustion of Lignocellulosic Materials in N<sub>2</sub>/O<sub>2</sub> and CO<sub>2</sub>/O<sub>2</sub> atmospheres. *Bioresour. Technol.*, **107**, 444–450.
- Lai, Z.; Ma, X.; Tang, Y.; Lin, H. (2012b) Thermogravimetric Analysis of the Thermal Decomposition of MSW in N<sub>2</sub>, CO<sub>2</sub> and CO<sub>2</sub>/N<sub>2</sub> Atmospheres. *Fuel Process. Technol.*, **102**, 18–23.
- Li, Q.; Zhao, C.; Chen, X.; Wu, W.; Li, Y. (2009) Comparison of Pulverized Coal Combustion in Air and in O<sub>2</sub>/CO<sub>2</sub> Mixtures by Thermo-Gravimetric Analysis. *J. Anal. Appl. Pyrol.*, **85**, 521–528.
- Liao, Y.; Ma, X. (2010) Thermogravimetric Analysis of the Co-Combustion of Coal and Paper Mill Sludge. *Appl. Energy*, **87**, 3526–3532.
- Liu, G.; Liao, Y.; Guo, S.; Ma, X.; Zeng, C.; Wu, J. (2016) Thermal Behavior and Kinetics of Municipal Solid Waste During Pyrolysis and Combustion Process. *Appl. Therm. Eng.*, **98**, 400–408.
- Minkova, V.; Marinov, S. P.; Zanzi, R.; Bjornbom, E.; Budinova, T.; Stefanova, M.; Lakov, L. (2000) Thermochemical Treatment of Biomass in a Flow of Steam or in a Mixture of Steam and Carbon Dioxide. *Fuel Process. Technol.*, **62**, 45–52.
- Molina, A.; Shaddix, C. R. (2007) Ignition and Devolatilization of Pulverized Bituminous Coal Particles During Oxygen/Carbon Dioxide Coal Combustion. *Proc. Combust. Inst.*, **31**, 1905–1912.
- Otero, M.; Gómez, X.; García, A. I.; Morán, A. (2007) Effects of Sewage Sludge Blending on the Coal Combustion: A Thermogravimetric Assessment. *Chemosphere*, **69**, 1740–1750.
- Patel, H.; Pandey, S. (2012) Evaluation of Physical Stability and leachability of Portland Pozzolona Cement (PPC) Solidified Chemical Sludge Generated from Textile Wastewater Treatment Plants. *J. Hazard. Mater.*, **207–208**, 56–64.
- Peng, X.; Ma, X.; Lin, Y.; Guo, Z.; Hu, S.; Ning, X.; Cao, Y.; Zhang, Y. (2015a) Co-Pyrolysis Between Microalgae and Textile Dyeing Sludge by TG-FTIR: Kinetics and Products. *Energ. Convers. Manage.*, **100**, 391–402.
- Peng, X.; Ma, X.; Xu, Z. (2015b) Thermogravimetric Analysis of Co-Combustion Between Microalgae and Textile Dyeing Sludge. *Bioresour. Technol.*, **180**, 288–295.
- Selcuk, N.; Yuzbasi, N. S. (2011) Combustion Behaviour of Turkish Lignite in O<sub>2</sub>/N<sub>2</sub> and O<sub>2</sub>/CO<sub>2</sub> Mixtures by using TGA-FTIR. *J. Anal. Appl. Pyrol.*, **90**, 133–139.

- Singh, D.; Croiset, E.; Douglas, P. L.; Douglas, M. A. (2003) Techno-Economic Study of CO<sub>2</sub> Capture from an Existing Coal-Fired Power Plant: MEA Scrubbing vs. O<sub>2</sub>/CO<sub>2</sub> Recycle Combustion. *Energ. Convers. Manage.*, **44**, 3073–3091.
- Sun, B.; Yu, J.; Tahmasebi, A.; Han, Y. (2014) An Experimental Study on Binderless Briquetting of Chinese Lignite: Effects of Briquetting Conditions. *Fuel Process. Technol.*, **124**, 243–248.
- Zhang, H.; He, P.; Shao, L. (2008) Fate of Heavy Metals During Municipal Solid Waste Incineration in Shanghai. *J. Hazard. Mater.*, **156**, 365–373.
- Zhuo, Z.; Liu, J.; Sun, S.; Sun, J.; Kuo, J.; Chang, K.; Fu, J.; Wang, Y. (2017) Thermogravimetric Characteristics of Textile Dyeing Sludge, Coal and their Blend in N<sub>2</sub>/O<sub>2</sub> and CO<sub>2</sub>/O<sub>2</sub> Atmospheres. *Appl. Therm. Eng.*, **111**, 87–94.